Climate Dynamics (2001) 17: 795–809

S. K. Gulev · O. Zolina · S. Grigoriev

Extratropical cyclone variability in the Northern Hemisphere winter from the NCEP/NCAR reanalysis data

Received: 7 July 2000 / Accepted: 30 November 2000

Abstract The winter climatology of Northern Hemisphere cyclone activity was derived from 6-hourly NCEP/NCAR reanalysis data for the period from 1958 to 1999, using software which provides improved accuracy in cyclone identification in comparison to numerical tracking schemes. Cyclone characteristics over the Kuroshio and Gulfstream are very different to those over continental North America and the Arctic. Analysis of Northern Hemisphere cyclones shows secular and decadal-scale changes in cyclone frequency, intensity, lifetime and deepening rates. The western Pacific and Atlantic are characterized by an increase in cyclone intensity and deepening during the 42-year period, although the eastern Pacific and continental North America demonstrate opposite tendencies in most cyclone characteristics. There is an increase of the number of cyclones in the Arctic and in the western Pacific and a downward tendency over the Gulf Stream and subpolar Pacific. Decadal scale variability in cyclone activity over the Atlantic and Pacific exhibits south-north dipole-like patterns. Atlantic and Pacific cyclone activity associated with the NAO and PNA is analyzed. Atlantic cyclone frequency demonstrates a high correlation with NAO and reflects the NAO shift in the mid 1970s, associated with considerable changes in European storm tracks. The PNA is largely linked to the eastern Pacific cyclone frequencies, and controls cyclone activity over the Gulf region and the North American coast during the last two decades. Assessment of the accuracy of the results and comparison with those derived using numerical algorithms, shows that biases inherent in numerical procedures are not negligible.

S. K. Gulev (✉) · O. Zolina · S. Grigoriev
P.P. Shirshov Institute of Oceanology, RAS,
36 Nakhimovsky ave., 117218 Moscow, Russia
E-mail: gul@gulev.sio.rssi.ru

1 Introduction

The intensity of synoptic processes is usually characterized by variances of the band-passed synoptic time series of sea level pressure (SLP) or the height of a reasonably chosen geopotential level (e.g., 500 hPa), available from model data, operational analyses and reanalyses (Blackmon et al. 1984; Trenberth 1991; Ayrault et al. 1995; Branstator 1995; Christoph et al. 1997; Rogers 1997). These band-passed statistics have been used to identify storm track modes associated with phenomena such as the North Atlantic Oscillation (NAO) (Rogers 1997), to analyze changes in storm activity induced by antropogenic greenhouse effects (Schubert et al. 1998; Carnell and Senior 1998; Carnell et al. 1996; Ulbrich and Christoph 1999) and for other purposes. However, this approach has several limitations. Synoptic activity on different time scales may exhibit different patterns of interannual variability (Ayrault et al. 1995; Gulev 1997; Gulev et al. 2000). Moreover, the consideration of synoptic variances does not allow for analysis of characteristics of individual cyclones, such as deepening rates, lifetimes, and propagation velocities. An alternative approach is to track individual cyclones, using sub-daily SLP analyses.

Storm tracking historically started with manual procedures. Later, different authors developed a number of numerical schemes, designed for application to model data or climatological archives (Alpert et al. 1990b; Le Treut and Kalnay 1990; Murray and Simmonds 1991; Jones and Simmonds 1993; Koenig et al. 1993; Hodges 1994; Sinclair 1994, 1997; Serreze 1995; Serreze et al. 1997; Blender et al. 1997; Sinclair and Watterson 1999). These schemes find the cyclone centers and link them on sequential snapshots, tracking the life cycle of individual systems. Tracking is the main source of uncertainties inherent in numerical schemes. Most problems appear when fast wave-type cyclones overrun stationary lows, or when multi-center depressions are identified. Consideration of limited areas (e.g., Mediterranean Sea)

(Alpert et al. 1990a, b; Trigo et al. 1999) increases the accuracy of tracking, but leads to biases in the counts of cyclones that are generated or decay out of the study region. Storm count algorithms represent simplified versions of numerical tracking schemes. They count the occurrences of the cyclone centers at grid points (Schinke 1993; Stein and Hense 1994; Lambert 1996). These algorithms do not track the cyclones, and hence do not allow for analysis of individual life cycles, i.e., they are similar in this sense to analysis of band-passed series.

Manual tracking is more accurate in comparison to numerical procedures, because an experienced operator can better assess synoptically complex situations. Nevertheless, manual procedures are also prone to random errors in cyclone identification and to mistakes in digitizing. Moreover, manual tracking requires considerable time, and this is the main reason why the less accurate numerical tracking is preferred. We present in this study a 42-year climatology of cyclone characteristics over the Northern Hemisphere derived from the NCEP/NCAR reanalysis, using an interactive storm tracking procedure. It is based on the computer animation of SLP fields and combines the advantages of numerical and manual approaches. In Sect. 2 we discuss the data and the method used to track cyclones. Section 3 examines the climatology of cyclone characteristics and regional features in cyclone life cycle. Secular changes and interannual variability in cyclone parameters are considered in Sect. 4. Section 5 summarizes the results in the context of possible recent changes in the atmospheric circulation regimes. In an Appendix we address the issue of the accuracy of the tracking algorithm.

2 Data and methods

Storm statistics derived from gridded SLP data depend on the quality of the analyses used. They may be influenced by the changing data coverage and analysis techniques, resulting in artifacts in cyclone characteristics (Agee 1991; Ueno 1993; von Storch et al. 1993). Recently the National Centers for Environmental Prediction (NCEP) has produced a dynamically consistent synoptic scale resolution data set of basic atmospheric quantities and computed parameters, known as NCEP/NCAR reanalysis (Kalnay et al. 1996). We used 6-hourly NCEP/NCAR SLP fields on a 2.5 by 2.5° grid for the Northern Hemisphere for the period 1958–1999. These data are considered to be instantaneous values at the reference time. We considered the winter period from January to March. Selection of the "cold" season from October–November to March (e.g., Blender et al. 1997) results in mixing of features of the autumn and winter seasons. Osborn et al. (1999) used DJFM as the winter season. However, the cross-correlations between the monthly anomalies within the JFM period are much higher than those between the December and January/February anomalies.

Cyclone characteristics assessed from the NCEP/NCAR reanalysis may be influenced by time dependent biases inherent in numerical weather prediction products. Although the data assimilation system of the NCEP/NCAR reanalysis is frozen, assimilation input changed during the last four decades. White (2000) reported that trends in some variables (e.g., sea-air fluxes in the Southern Hemisphere) of the NCEP/NCAR reanalysis are correlated with the number of observations. Records of SLP are considered to be more homogeneous. In the North Atlantic and North Pacific the termination of observations at Ocean Weather Stations (OWS) in the early 1970s was partly compensated by the establishment of (National Data Buoy Center) NDBC and (Japan Meteorological Agency) JMA buoys. Inspection of the number of SLP reports in the COADS data set shows about 5% decrease in the number of observations in the 1980s and 1990s in comparison to earlier decades. However, for the North Atlantic and North Pacific midlatitudes the number of reports remains large enough and should not affect cyclone statistics. Recently (NCEP 2000) a problem has been discovered in the encoding of SLP data in the NCEP/NCAR reanalysis, that affects the period upto 1967. The problem results in unphysically high SLP values (>1050 hPa). However, these data were rejected from the analysis (NCEP 2000), and no erroneous data were used. However, the omission could affect the data assimilation system and introduce some biases in the mid latitudes.

The storm tracking was performed using software of Grigoriev et al. (2000), which is based on computer animation of the SLP fields and simulates the manual procedure, but makes it faster and less dependent on the subjective view and mistakes of a particular operator. When the cyclone centers are defined, the tracking is carried out by an interactive friendly dialogue. The output for each cyclone track (coordinates, date/time, and the corresponding SLP values) is saved in the background of animation for the further analysis. Pressure minima were defined with respect to the eight neighboring grid points. This is superior to identification of a minimum with respect to four grid points (Lambert 1996) or using the average SLP over the nine grid points minus a prescribed value, usually 2 hPa (Serreze et al. 1993; Serreze 1995). Only cyclones which at least once were deeper than 1000 hPa were analyzed. On the one hand, this eliminates a considerable number of shallow cyclones from the analysis; on the other hand, this increases the accuracy of tracking. All cyclones with a lifetime shorter than 12 h were excluded from analysis.

From the tracking results we computed cyclone frequencies and life cycle characteristics. Mapping the results is the source of a number of uncertainties, connected with the choice of the effective box size (Hayden 1981a, b; Taylor 1986). This problem has a smaller impact on the cyclone climatology derived for limited areas, say for the North American coast (Hayden 1981a, b) or the Arctic basin only (Serreze and Barry 1989), when the results can be either area-normalized or performed initially over the equal-area grid. For hemispheric scale tracking, it is necessary to account not only for the decrease in area of an n by n degree box with latitude, but also for the preferential directions of cyclone propagation, which is very important in the high latitudes. In our study, results south of 70°N are presented for 5° boxes. The grid cells north of 70°N were chosen according to the recommendations of Taylor (1986) who emphasized the importance of the cell orientation with respect to the direction that the storms are traveling. This high-latitudinal counterpart of the 5 by 5° basic grid provides the most effective catchment of cyclones in the Arctic basin. It starts with the latitude circle at 84°N and then uses the boxes with longitudinal dimensions of 30° (84°N–80°N), 24° (80°N–75°N), and 20° (75°N–70°N). This grid avoids the biases associated with fast cyclones which pass one or more boxes during one time step (Chandler and Jonas 1999). These biases tend to underestimate storm counts and are mostly pronounced in high latitudes.

3 Winter climatology of the Northern Hemisphere cyclone activity

Cyclone frequencies were computed as the occurrences of cyclone centers in the selected squares, normalized with respect to the square of the 5-degree box at 45°N (approximately 218 000 km^2). Figure 1a shows mean climatological winter storm frequencies for the period from 1958 to 1999. The primary North Pacific and North Atlantic storm tracks align from the Kuroshio

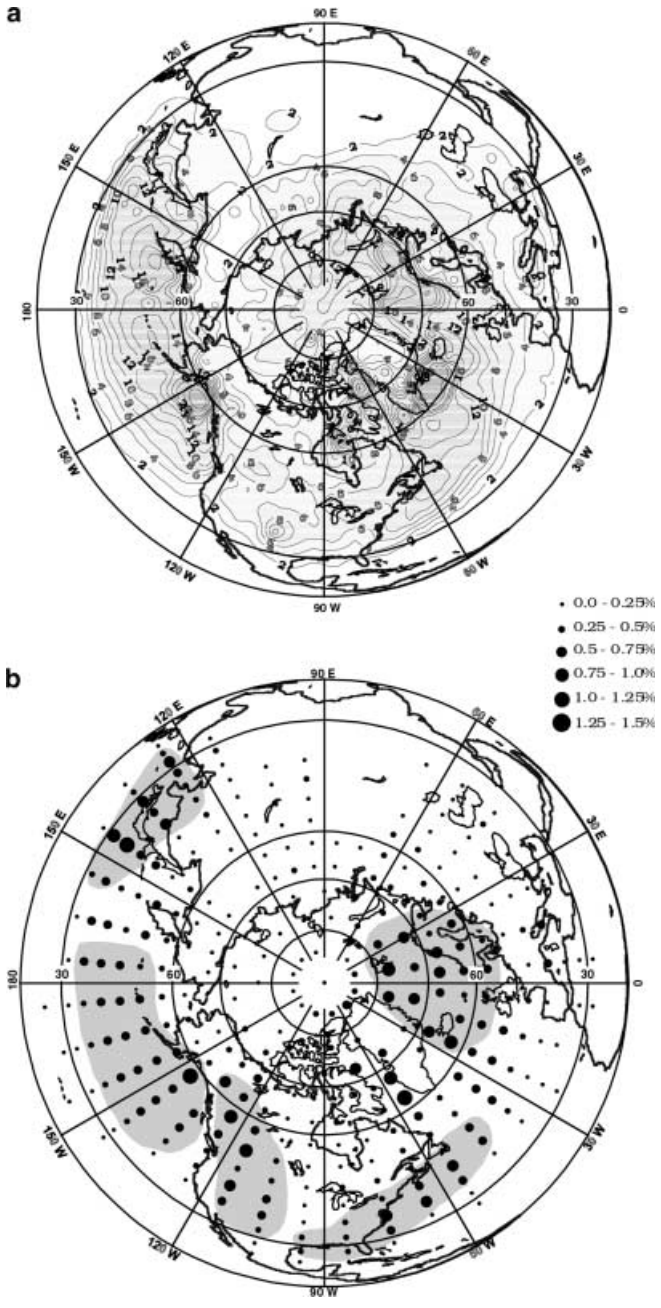

Fig. 1 **a** Climatological winter cyclone frequency (events/winter per 218 000 km^2) for the Northern Hemisphere and **b** climatological winter frequency of cyclone generation (percent of the total number of cyclones)

region to the Gulf of Alaska, and from the North American coast to the Arctic respectively. Over the Gulf Stream, Kuroshio, Gulf of Alaska, and over the Greenland and Barents Seas frequencies are from 12 to 20 events per winter. Many authors have analyzed cyclone frequencies using different procedures of storm identification, different data and different mapping approaches (Reitan 1974; Zishka and Smith 1980; Whittaker and Horn 1981; Bell and Bosart 1989; Serreze et al. 1993; Lambert 1996, and others) making quantitative comparisons difficult. Nevertheless, Fig. 1a shows qualitative agreement with most other results. We estimated the cyclone frequency for the IL (Iceland Low) region investigated by Serreze et al. (1997) and found that the mean JFM frequency integrated over this region is about 10% higher than shown in that study.

The frequency of cyclogenesis (i.e., the first observation of each cyclone) (Fig. 1b) was computed in the same manner as cyclone frequency. Areas with the most intensive cyclone generation cover about 10% of the Northern Hemisphere and account for 50% of cyclogenesis events. Most cyclogenesis events occur over the Kuroshio in the Pacific (10% of all generation events) and near the subtropical North American coast (7%). Storm generation is also frequent in the eastern Pacific (12%), near southeast Greenland and in the Barents Sea (11%). Cyclogenesis over the North American continent is less common than in the primary storm formation regions. Cyclogenesis over the Great Lakes, frequently considered one of the major sources of the Atlantic cyclones, is considerably weaker than over the Rocky Mountains and eastern North American coast. The eastern Mediterranean is responsible for the generation of about 3% of cyclones. The mean climatological number of cyclones over the Northern Hemisphere is 234 per winter. On average, 99 of them were generated and propagated over the Pacific sector, and about 130 over the Atlantic sector including the Arctic (sectors were separated by the longitude 120°W). The climatological number of Arctic cyclones, defined as those that crossed 65°N, is 50.

Cyclones may be characterized by intensity (i.e., maximum depth), lifetime, and deepening rates. Lifetime was estimated as the number of 6-hourly steps between the cyclone generation and decay. Taking into account that cyclones could occur earlier and decay later, our estimates of the lifetime may be underestimated by approximately 6 h. Following Roebber (1984, 1989) and Serreze (1995), deepening/filling rates were normalized as $\langle \delta p \rangle = \delta p(\sin \phi_{ref}/\sin \phi)$, where ϕ_{ref} is a reference latitude, taken as 45° in this study. This geostrophic adjustment accounts for a latitude-dependent storm vorticity change. The average deepening rates were estimated for the time of cyclone deepening, and the maximum deepening was derived taking the largest pressure falls between time steps (Sanders and Gyakum 1980; Sanders 1986).

Figure 2 shows climatological histograms of cyclone depth, deepening/filling rates, and life time. Modal maximum depth ranges from 990 to 995 hPa. About 20% of cyclones over the Northern Hemisphere are deeper than 970 hPa (known as intense events). Histograms for different regions (Fig. 3a, b) show that for cyclones generated in the western Pacific and over the Gulf Stream modal maximum depth ranges from 960 to 980 hPa, with intense events accounting for about 40% of cases. For the eastern Pacific modal intensity is from 980 to 990 hPa, and less than 15% of cyclones are extreme events. For the Arctic, modal maximum depth

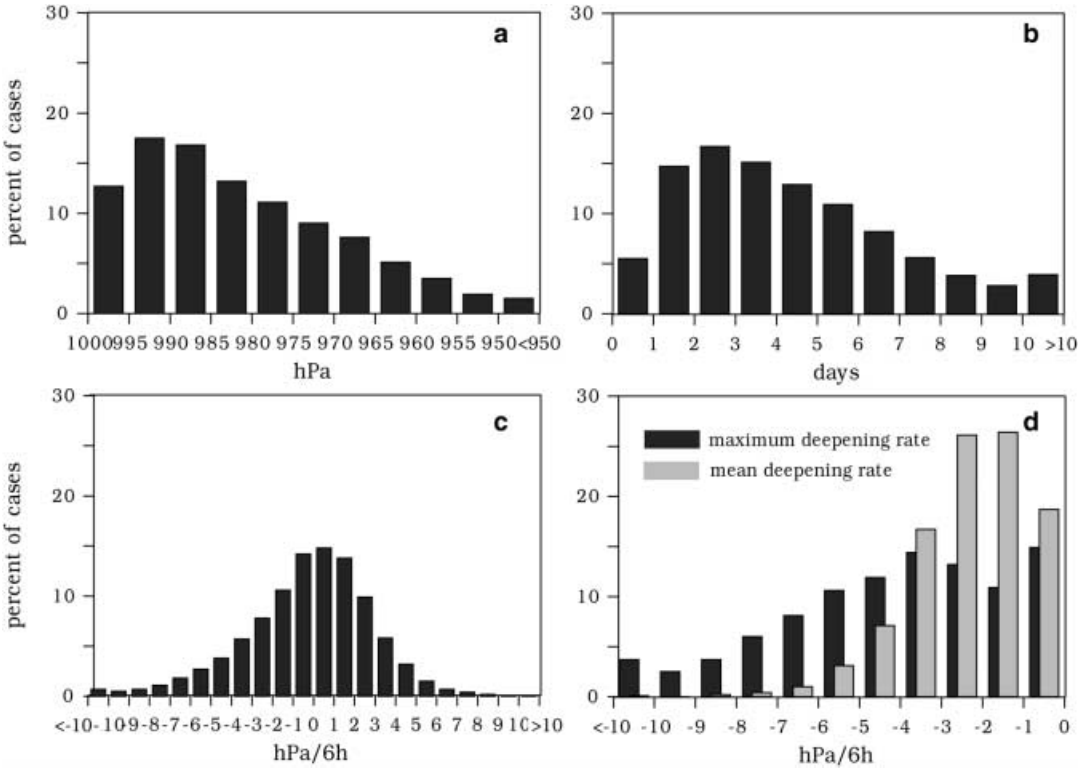

Fig. 2a–d Winter climatological occurrence histograms of **a** cyclone intensity, **b** lifetime, **c** deepening/filling rates, and **d** mean and maximum deepening rates for the phase of cyclone intensification for the Northern Hemisphere

is from 970 to 990 hPa, accounting for about 55% of cyclones. About 20% are intense events, considerably fewer than in midlatitudinal Atlantic and Pacific. Cyclones generated over the North American continent demonstrate very different statistics of intensity that are typical for orographic cyclogenesis (Tibaldi et al. 1990). Nearly 40% have a maximum depth exceeding 990 hPa. The number of the intense events (18%) is considerably smaller in comparison to the cyclones found over the Kuroshio and Gulf Stream curve.

The modal hemispheric life time is 2–3 days (Fig. 2b), and 50% of all cyclones exist from one to four days. However, 17% of cyclones are long-living, with lifetimes longer than seven days. About 60% of cyclones generated over the Kuroshio exist from 4 to 8 days and nearly a quarter have lifetimes exceeding 8 days (Fig. 3c). Cyclones with a lifetime less than two days represent only 5% of cases. In the eastern Pacific the modal lifetime is much shorter (2 to 4 days). More than 60% of cyclones in the Atlantic exist from 2 to 6 days with the mean lifetime of about four days. The Arctic region is characterized by the shortest cyclone lifetimes with a mean of less than three days. This may result from the contribution of the short-living polar mesocyclones (e.g., Harold et al. 1999), although only few of them can be resolved by the NCEP/NCAR reanalysis which has a coarser resolution than ECMWF analyses used by Harold et al. (1999). Although North American continental cyclones (Fig. 3d) demonstrate a mean lifetime from 2 to 4 days, 21% of them exist for longer than eight days. Note that most long-lived (more than 10 days) cyclones are primarily generated over North America (8% of all cyclones).

The climatological hemispheric histogram of cyclone deepening/filling rates is shown in Fig. 2c. One third of deepening events are less than 3 hPa per 6 h, and about 10% are intense deepening events (more than 6 hPa per 6 h) is about 10%. In order to analyze deepening for individual cyclones, it is more effective to consider mean and extreme deepening rates during the phase of cyclone intensification rather than the overall statistics of deepening rates. Figure 2d shows hemispheric histograms for the mean and maximum (during 12-hourly time periods) deepening rates. The mean deepening of 65% of cyclones is less than 3 hPa per 6 h and only for 2% of cyclones does the mean deepening exceed 6 hPa per 6 h. Cyclones generated over the Kuroshio (Fig. 3e) are characterized by greater mean deepening than in the eastern Pacific (mean deepening rates are 3.3 and 2 hPa per 6 h, respectively). Atlantic cyclones exhibit higher mean deepening rates (3–4 hPa per 6 h) in comparison to continental (2–3 hPa per 6 h) and Arctic cyclones (1–2 hPa per 6 h) (Fig. 4f). Roebber (1989) also reported pronounced differences in deepening rates for the oceanic and continental cyclones.

Analysis of maximum deepening rates (Fig. 3d) shows that 17% of all cyclones are rapidly intensifying. Rapid deepening is an outstanding feature of oceanic cyclones (Sanders and Guakum 1980; Rogers and Bosart 1986; Uccellini 1990). Figure 4g, h shows rapid

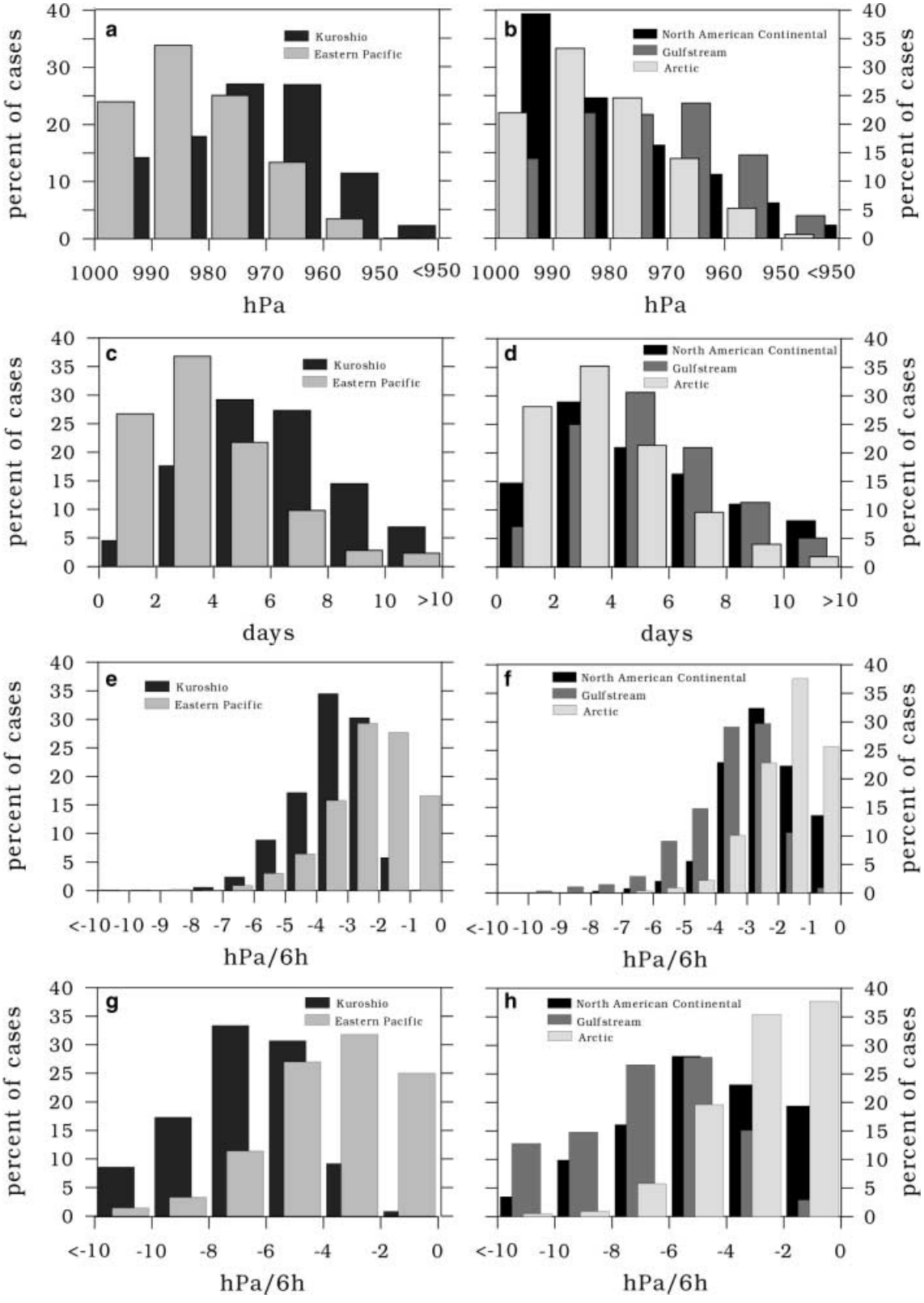

Fig. 3a–h Winter climatological occurrence histograms of **a, b** cyclone intensity, **c, d** lifetime, **e, f** mean and **g, h** maximum deepening rates for cyclones generated over the Kuroshio and in the eastern Pacific (**a, c, e, f**) and over North America, Gulf Stream and in the Arctic (**b, d, f, h**)

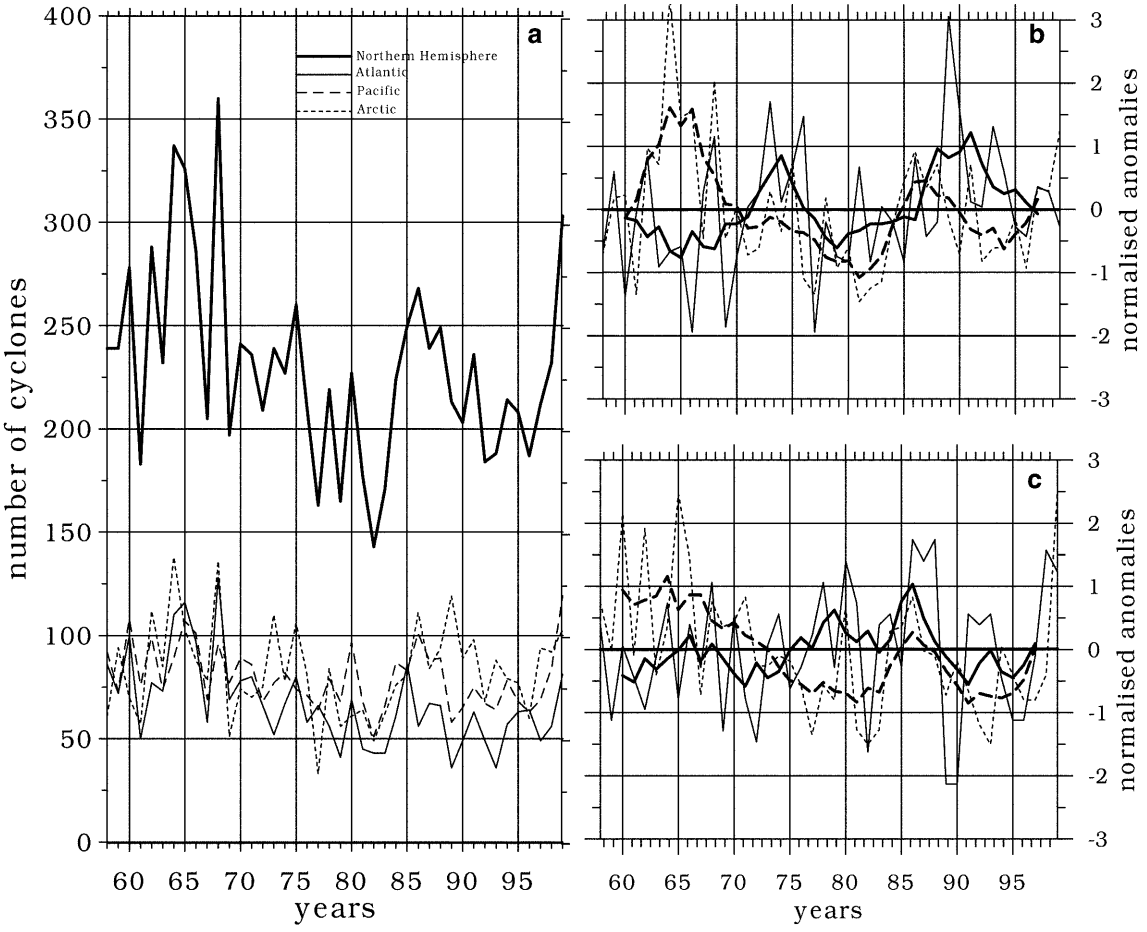

Fig. 4a–c Time series of **a** the total winter number of cyclones over the Northern Hemisphere (*bold line*), Pacific (*thin line*), Atlantic (*dashed line*), and Arctic (*dotted line*), and normalized anomalies of the number of cyclones with the intensity less than 980 hPa (*solid line*) and from 980 to 1000 hPa (*dotted line*) in **b** Arctic and **c** Pacific

deepening for 50% of cyclones generated over the Kuroshio and Gulf Stream. Rapidly deepening cyclones represent 15%, 8% and 20% of cases in the eastern Pacific, Arctic and over North America respectively. These estimates were derived for the regions responsible for 50% of cyclones. Estimates for all cyclones over the Atlantic and Pacific are somewhat smaller (26% and 12% for the Kuroshio and Gulf Stream respectively). Some authors (e.g., Stewart and Donaldson 1989; Yau and Jean 1989) define rapid deepening using 24-hourly pressure falls. Analysis of 24-hourly SLP falls shows that 19% of the Atlantic cyclones and 10% of the Pacific cyclones can be defined as meteorological "bombs" with a deepening of 24 hPa per 1 day.

4 Interannual variability of cyclone characteristics

4.1 Secular changes in the cyclone frequencies

Hemispheric and regional time series of the total number of cyclones are shown in Figure 4a. Figure 4b, c presents anomalies of the number of cyclones of different intensities for the Arctic and Pacific normalized by standard deviation. Despite pronounced interannual variability, secular changes in the number of cyclones are evident for the whole Northern Hemisphere and individual basins, demonstrating a downward tendency, mostly pronounced over the Atlantic and Pacific Oceans. Table 1 shows corresponding linear trends and their statistical significance according to a Student *t*-test. For the Northern Hemisphere the total number of cyclones has a downward tendency of 12 cyclones per decade. This trend is provided by the relatively shallow systems with central pressures of 980 to 1000 hPa, demonstrating a decrease of 13 cyclones per decade. Simmonds and Keay (2000) recently reported significant downward trends

Table 1 Estimates of linear trends (events per decade) in the number of cyclones of different intensity for different regions together with statistical significance (*t*-test)

Intensity	Northern Hemisphere	Atlantic sector	Pacific sector	Arctic
All cyclones	−12.4**	−8.9***	−3.3*	−0.2
980–1000 hPa	−13.1**	−6.2***	−4.0**	−2.8
< 980 hPa	0.7	−2.7***	0.7	2.7*

*P = 90% level; **P = 95% level; ***P = 99% level

also in the Southern Hemisphere cyclogenesis in the NCEP/NCAR reanalysis. Trends in the number of the Atlantic and Pacific cyclones are similar to those found for the Northern Hemisphere (−9 and −3.3 cyclones per decade respectively). In the Atlantic significant downward trends occur in the number of both relatively shallow and intense cyclones. In the Arctic deep cyclones demonstrate a slight increase of three cyclones per decade which is significant at the 90% level. The total number of the Arctic cyclones decreased in the 1960s and early 1970s and increased by 14 cyclones per decade from the late 1970s to 1990s. The number of cyclones in the Arctic and Atlantic have opposing tendencies for the last three decades. This is in agreement with Serreze et al. (1997) who reported increasing cyclone counts north of 60°N and the decrease in the latitudinal belt 30–60°N. Earlier estimates of trends in cyclone frequencies over the American continent (Reitan 1974; Zishka and Smith 1980) based on the data from the 1950s to 1970s, are in a qualitative agreement with our results for the same periods.

Figure 4b, c and Table 1 show that downward tendencies are primarily associated with the shallow systems. Deep cyclones at least in the Pacific and Arctic show weak positive trends. The exception is the Atlantic sector, where downward changes are found for both deep and shallow cyclones, although the magnitudes of trends in the number of relatively deep events is 2.5 times smaller in comparison with that for the shallow systems. There is also some indication of anticorrelation in the

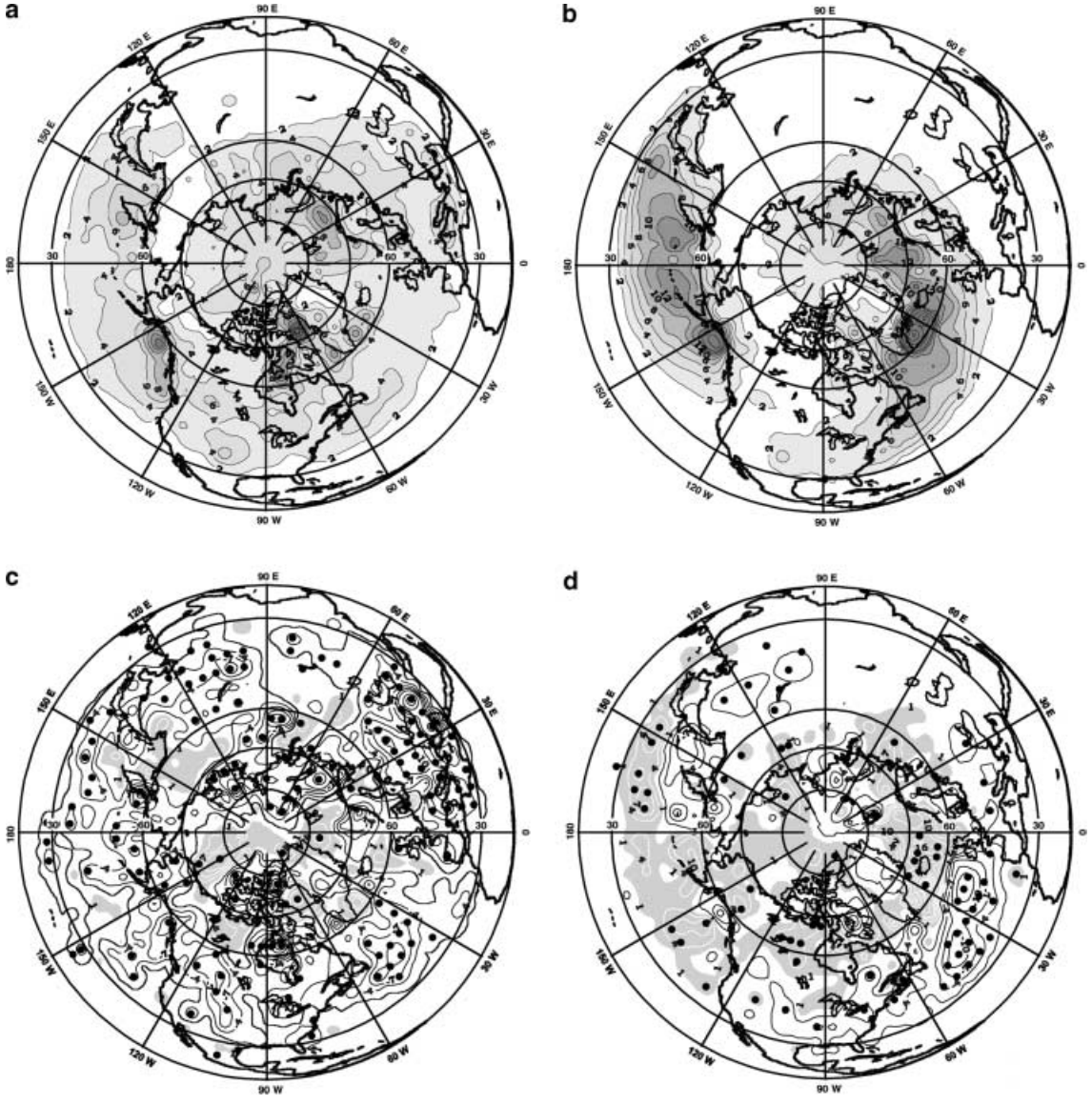

Fig. 5a–d Climatological winter cyclone frequency for cyclones with an intensity from **a** 980 to 1000 hPa and **b** less than 980 hPa, and estimates of linear trends in cyclone frequency (events per decade) for cyclones with an intensity **c** from 980 to 1000 hPA and **d** less than 980 hPa. *Black circles* indicate 95% significance (*t*-test)

numbers of deep and relatively shallow systems on interannual to decadal time scales. This is particularly pronounced in the Arctic in the 1960s, late 1980s, and 1990s. Figure 5a, b shows the frequencies of cyclones with intensity ranging from 980 to 1000 hPa (57% of events) and less than 980 hPa (43% of events). For shallow cyclones, storm tracks align more zonally in comparison to the pathways of intense events, characterized by a pronounced poleward deflection. Local frequency maxima for the shallow cyclones are found in the eastern Pacific, North America, Mediterranean, and the south of Europe. Frequency maxima of intense cyclones are located over the Kuroshio and Gulf Stream and in the Icelandic Low region. Figure 5c, d shows linear trends in the frequency of cyclones of different intensities and their statistical significance (*t*-test). Shallow cyclones demonstrate primarily negative trends which are significant in the western Pacific, western Atlantic and over the southern Europe (10 to 15 cyclones per decade). Significant upward tendencies are observed in the Labrador Sea and Canadian Arctic. Positive trends in the frequency of intense events (Fig. 5d) are significant in the Kuroshio region and mid-latitude Pacific. Weak negative trends are observed over the Okhotsk and Bering seas. Over the Atlantic we find weak negative trends in mid latitudes and statistically significant upward trends of about 15–20 cyclones per decade in the Iceland Low region and European Arctic. Thus, secular tendencies in the intense cyclogenesis indicate south–north dipole patterns, which are reversed with respect to each other in the Atlantic/Arctic sector and in the Pacific.

4.2 Variability in the characteristics of the cyclone life cycle

In order to analyze interannual to decadal scale changes in cyclone life cycle, we evaluated what we term occurrence anomalies. First, histograms (as in Figs. 2, 3) were computed for every individual winter. Averaging gives climatological mean probability density distributions in reasonable agreement with those presented in Fig. 2. Then we derived the frequency anomalies for every winter with respect to the mean climatological histogram and normalized them by scaling with interannual standard deviations (*std*) of the frequency for the selected bins: $\boldsymbol{P}'(x) = [\boldsymbol{P}(x) - \langle \boldsymbol{P}(x) \rangle]/\sigma[\boldsymbol{P}(x)]$, where x is the analyzed parameter (e.g. maximum depth), $\boldsymbol{P}(x)$ is probability density distribution for an individual winter, $\boldsymbol{P}'(x)$ is the normalized anomaly of the probability density distribution, and $\langle\ \rangle$ is the averaging operator. Figure 6a summarizes the interannual variability of the normalized frequency anomalies of maximum cyclone depth over the Northern Hemisphere smoothed with a 5-year running mean. There is a tendency for an increase in the frequency of deep cyclones during the 42-year period. Positive anomalies of the probability of shallow cyclones are apparent during the 1960s and 1970s, while intense events are characterized by negative anomalies. In the 1980s and 1990s intense cyclones become more frequent, while the number of weak cyclones decreases. This general tendency is pronounced for the storm formation regions over the Kuroshio and Gulf Stream and for Arctic cyclones. For the western Pacific there has been an increase in the number of deep cyclones in the late

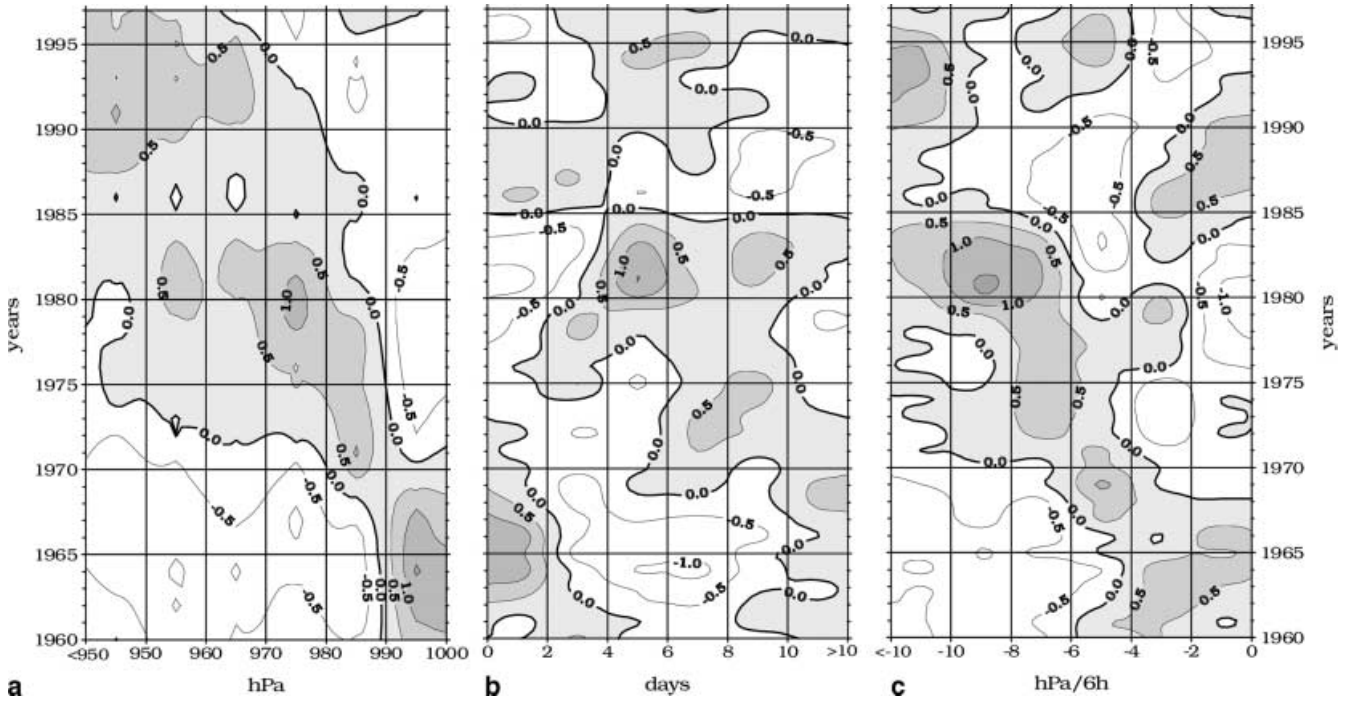

Fig. 6a–c Interannual evolution of the normalized occurrence anomalies of **a** the cyclone maximum depth, **b** lifetime and **c** maximum deepening rates over the Northern Hemisphere

1970s and a corresponding decrease in the occurrence of shallow cyclones.

The hemispheric anomalies reveal a general increase in the number of short-living cyclones at least from the early 1960s to the late 1980s, although there is a positive anomaly of the occurrence of very short-living cyclones in the 1960s (Fig. 6b). In the 1990s cyclone lifetime increased. The lifetime of cyclones generated over the Kuroshio and North America regions increased remarkably in the mid 1970s, although for the eastern Pacific there has been a decreasing lifetime over the 42-year period.

Interannual variability in the hemispheric statistics of the maximum deepening rate (Fig. 6c) indicates a considerable increase of the number of rapidly intensifying cyclones during the 42-year period. Although storm formation regions over the Gulf Stream and Kuroshio show pronounced increases of the number of rapidly deepening cyclones starting in the second part of the 1970s, continental cyclones show a weakening of deepening starting from the mid 1970s. Figure 7 shows time series of the number of rapidly intensifying cyclones for the three generation regions. Over the Kuroshio there is a secular increase in the number of rapidly deepening cyclones of approximately one event per decade and pronounced decadal variability. The numbers of rapidly deepening cyclones generated over the American continent and over the Gulf Stream are negatively correlated. Starting from the late 1970s positive anomalies of the number of rapidly deepening cyclones over the Gulf Stream are associated with primarily negative anomalies of the number of continental cyclones characterized by extreme deepening.

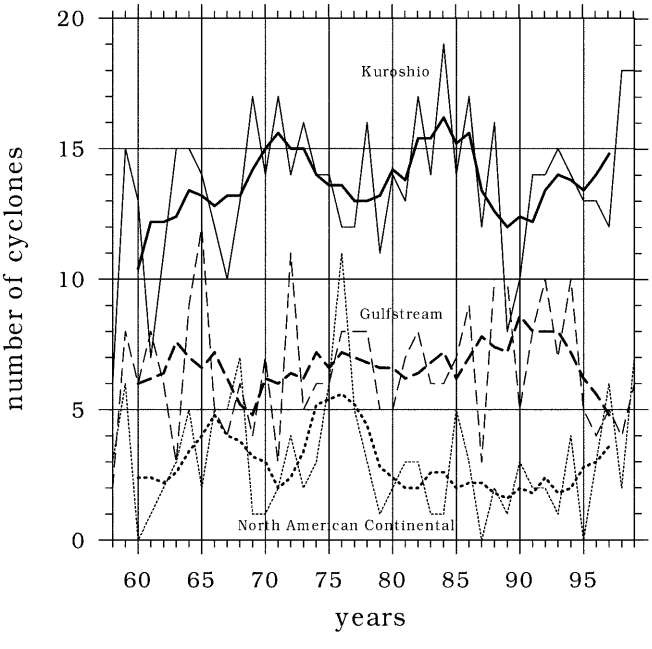

Fig. 7 Interannual changes in the number of rapidly intensifying cyclones, generated over the Kuroshio (*solid line*), Gulf Stream (*dashed line*) and continental North America (*dotted line*). *Bold lines* correspond to the 3-year running mean

4.3 EOF analysis of interannual variability

In order to depict patterns of interannual to quasi-decadal variability, we applied EOF analysis to the detrended anomalies of cyclone counts. EOFs were computed separately for the Atlantic/Arctic and Pacific sectors, which are defined in Fig. 8. For both Atlantic/Arctic and Pacific sectors only the first EOFs were well separated from the others. Figure 8a shows the spatial patterns of the first EOFs of the frequency of cyclones deeper than 980 hPa. The first EOFs account for 28 and 25% of the total variance in the Atlantic/Arctic and Pacific sectors respectively, and represent dipole-like patterns associated with the mid-latitudinal and subpolar storm tracks. In the Pacific, intensification of cyclone activity in the subtropics and mid latitudes corresponds to the weakening of cyclones propagating northeastward over the Okhotsk and Bering seas. In the Atlantic/Arctic sector intensification of continental and Arctic cyclones is associated with negative anomalies in cyclone activity over the Gulf Stream, mid-latitudinal Atlantic and south Europe. Dickson and Namias (1976) documented an out-of-phase behavior between North American continental and east coast cyclone counts. Figure 9a shows the corresponding normalized principal components (PCs) for the Pacific and Atlantic/Arctic sectors. From the 1950s to the mid 1970s there was a general similarity in the decadal scale variability of the first Atlantic and Pacific PCs. However, from the mid 1970s the Atlantic and Pacific modes demonstrate opposite tendencies.

We applied canonical correlation analysis (CCA) to the time series of intense cyclone frequencies in the Atlantic/Arctic and Pacific sectors. The intent is to identify spatial patterns that are optimally temporally correlated (von Storch and Zwiers 1999). For CCA we used the first five EOFs which account for 73% and 76% of the total variance in the Atlantic/Arctic sector and in the Pacific respectively. The results from the CCA remain stable with respect to different EOF truncations within the range of 3 to 8 EOFs. The first canonical pair, which indicates a correlation of 0.62 (Fig. 8b). The canonical pattern in the Atlantic/Arctic sector largely resembles the first EOF. The corresponding canonical pattern in the Pacific sector is described as an east-west dipole, centered at the Aleutian Low and the eastern midlatitudinal Pacific.

Storm track activity over the Northern Hemisphere is connected to the dominant patterns of atmospheric variability, such as the NAO and the North Pacific Oscillation (PNA). Positive anomalies of the NAO index (Rogers 1984; Barnston and Livezey 1987; Kushnir 1994; Hurrell 1995; Hurrell and van Loon 1997) are associated with the strengthening of the mid latitudinal westerly flow over the North Atlantic, and should lead to the intensification and poleward deflection of the North Atlantic midlatitudinal storm track. Serreze et al. (1997), using the data for 1964–1993, reported that the positive NAO phase is associated with more than a two-fold increase of cyclones in the Icelandic Low region and a

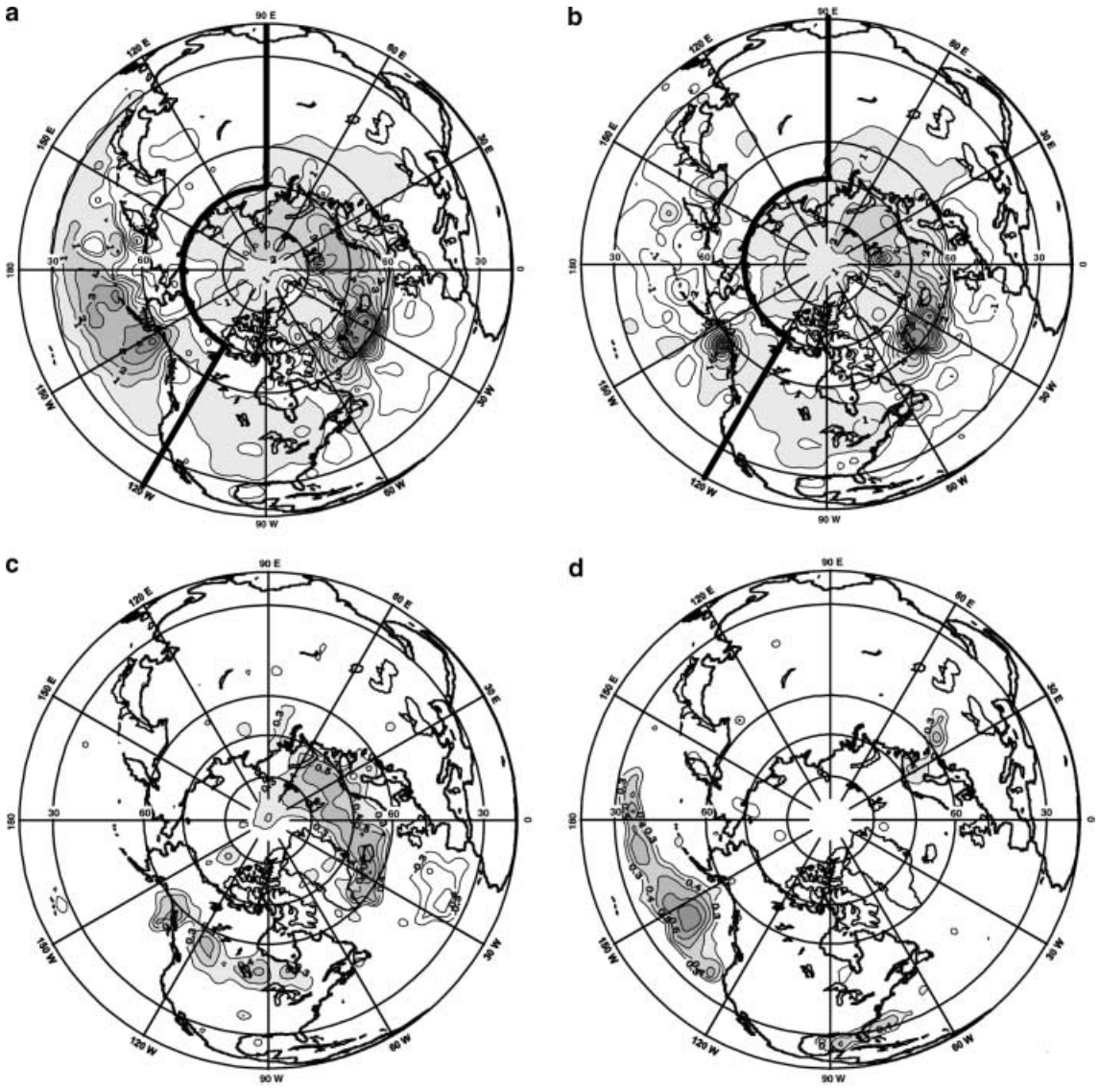

Fig. 8a–d First EOFs of the intense (< 980 hPa) cyclone frequency for the **a** Pacific and Atlantic/Arctic sectors, **b** first canonical patterns of cyclone frequencies in the Pacific and Atlantic/Arctic sectors, and associated correlation patterns between **c** the NAO and **d** PNA indices and the frequency of cyclones deeper than 980 hPa for the period 1958–1999

considerable decrease of storm frequency in the Atlantic subtropics and mid-latitudes. However, Rogers (1997) found that the North Atlantic storm track pattern is linked to the SLP dipole centered over the Bay of Biscay and the Barents Sea rather than to the NAO index. The PNA pattern is largely responsible for the strengthening and weakening of cyclogenesis in the eastern Pacific (e.g., Wallace et al. 1990; Barnston and Livezey 1987; Kushnir and Wallace 1989), and according to the model results of Christoph and Ulbrich (2000) may also have signatures in the Atlantic. Figure 9b, c shows the scatter plots between the NAO and PNA indices and the first normalized PCs of the cyclone frequency in the Atlantic/Arctic and Pacific sectors respectively. The correlation coefficient between the NAO and the dominant mode in the North Atlantic storm frequency is 0.86. In the Pacific the correlation with the PNA index is 0.68.

We computed associated correlations between the NAO and PNA indices and cyclone frequencies. Figure 8c, d shows correlation patterns of the frequency of cyclones deeper than 980 hPa with the NAO and PNA indices for the period 1958–1999. For the whole period the NAO index is positively correlated with cyclone activity over North America and the European Arctic. The highest correlation of 0.7 is found in the Icelandic Low region. Negative correlations are observed in the eastern subtropical and midlatitudinal Atlantic and reflect the intensification of cyclones propagating to southern Europe and the Mediterranean under the blocking high and Greenland anticyclone regimes, associated with a negative NAO. Associated correlation patterns of the cyclone frequency with the PNA index (Fig. 8d) largely resemble the first Pacific EOF (Fig. 8a) in showing the highest correlation (up to 0.74) in the eastern subtropical and

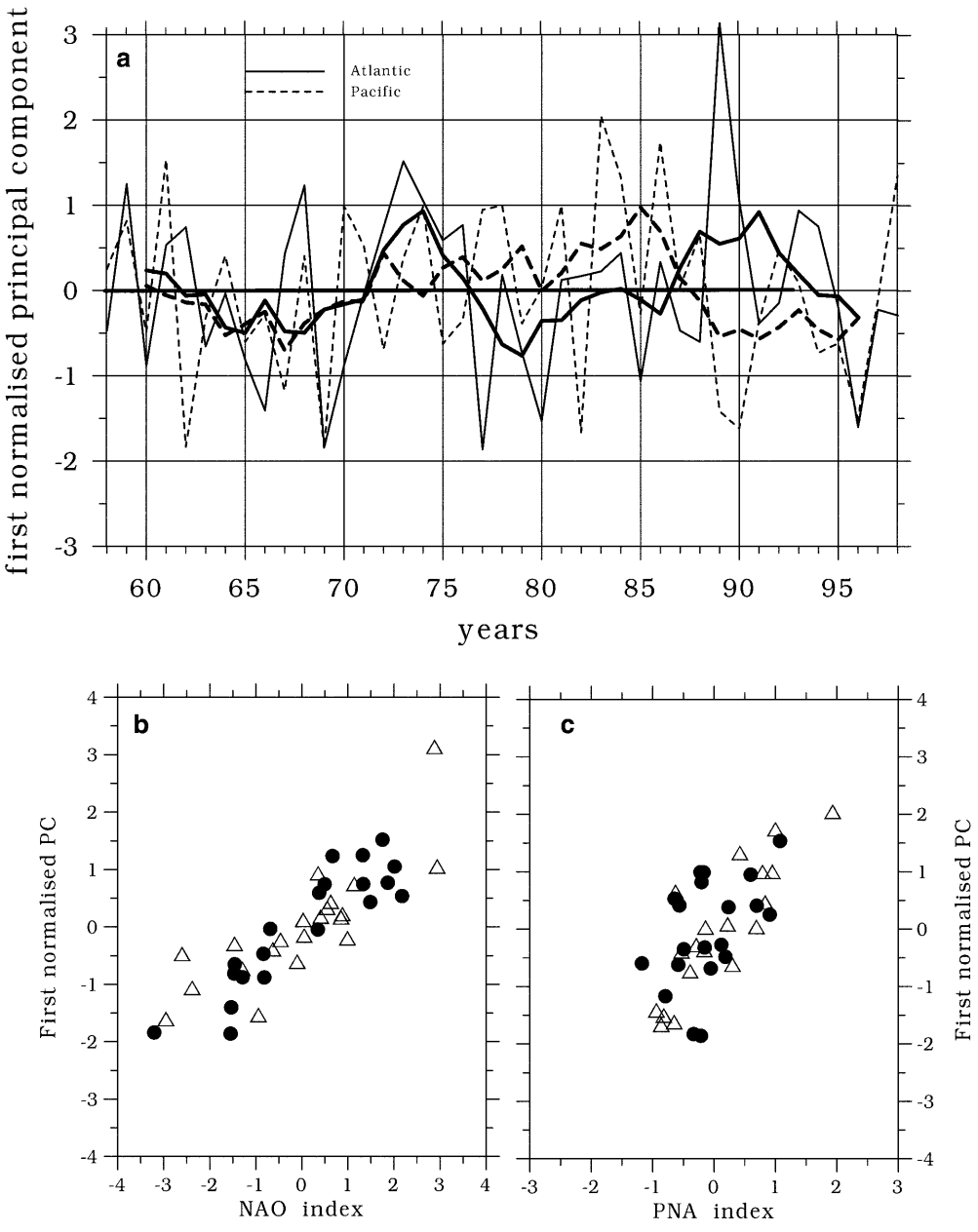

Fig. 9a–c First normalized principal components of the frequency of intense cyclones in the **a** Atlantic/Arctic (*solid line*) and Pacific (*dashed line*) sectors (*bold lines* correspond to the 5-year running mean), and scatter plots between **b** the NAO and **c** PNA indices and the first normalized PCs of cyclone frequency in the Atlantic/Arctic and Pacific sectors. *Black circles* and *open triangles* in *panels* **b, c** correspond to the periods 1958–1978 and 1979–1999 respectively

midlatitudinal Pacific. Another area of positive correlations is found in the Gulf of Mexico and the east North American coast. Thus, the PNA also has signatures in the subtropical Atlantic cyclone activity. Christoph and Ulbrich (2000) investigated this signal in the ECHAM4/OPYC3 model and argued that PNA can modify baroclinicity in the western Atlantic providing a low-level humidity transport from the Pacific.

5 Discussion

Sickmoeller et al. (2000) performed cyclone tracking over the Northern Hemisphere for 1979–1997 using the 1000 hPa geopotential height from the ECMWF reanalysis and the algorithm of Blender et al. (1997). They have found negative trends in the total number of cyclones over both the Pacific and Atlantic that agree with the results in Fig. 4 and Table 1. Storm frequency (termed by Sickmoeller et al. 2000 as *number of lows*) has increased over the Pacific, again in agreement with our results for intense events derived from a longer period from the NCEP/NCAR reanalysis (Fig. 5d). They found that the NAO index is highly correlated with the number of Atlantic stationary lows and that Pacific cyclone activity may have its counterpart in the Atlantic. In order to compare our results with those of Sickmoeller et al. (2000), we performed a separate analysis for the periods 1958–1978 and 1979–1999. Figure 9b, c show that for the North Atlantic the correlation between the NAO index and the first normalized PC of the cyclone frequency remains very high (0.9 and 0.81) for the periods

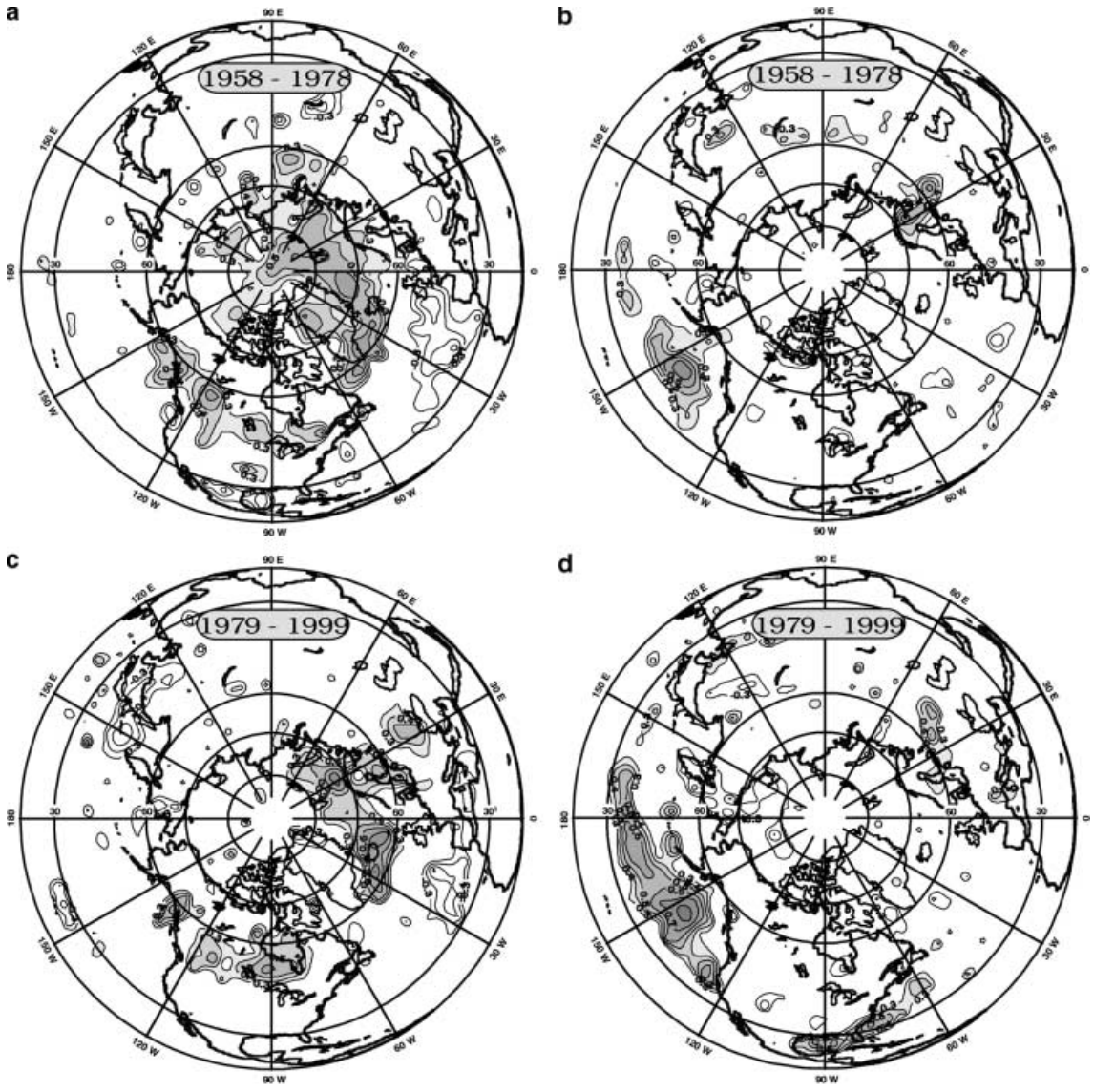

Fig. 10a–d Associated correlation patterns between **a, c** the NAO and **b, d** PNA indices and frequency of cyclones deeper than 980 hPa for the periods 1958–1978 (**a, b**) and 1979–1999 (**c, d**). Only significant (95%) correlations are contoured

1958–1978 and 1979–1999 respectively. However, in the Pacific the correlation between the PNA index and the first PC is much higher for the last two decades (0.84) in comparison to the period 1958–1978 (0.46).

Figure 10a, b and 10c, d shows the associated correlations between the NAO and PNA indices and cyclone frequencies for the periods 1958–1978 and 1979–1999. These periods are characterized by a southeastward shift of the correlation patterns over Europe and the Arctic. During 1958–1978 the NAO index shows a positive correlation with storm activity in the central and Canadian Arctic. Areas of the negative correlation depict the southmost location of the storm track over the eastern Atlantic and the region over the Gulf of Mexico and western Atlantic subtropics. During 1979–1999 positive correlations are located over the northern and eastern Europe and negative correlations are found over the Mediterranean. Hilmer and Jung (2000) demonstrated that the NAO dipole was shifted to the east in the late 1970s. A similar shift has been explored by Ulbrich and Christoph (1999) in a greenhouse gas experiment with the ECHAM4/ OPYC3 coupled model. Kodera et al. (1999) explained the switch between the NAO regimes in the 1950s–1970s and in 1980s–1990s by the growing impact of the polar night jet on the atmospheric variability during the last two decades. Our results show that the Atlantic cyclone frequencies reflect well the NAO shift in the late 1970s found by Hilmer and Jung (2000) and Kodera et al. (1999) in NCEP/NCAR data and by Ulbrich and Christoph (1999) in the model simulations.

The eastern Pacific pattern is more pronounced for the period 1979–1999, in comparison to the 1960s and 1970s (Fig. 10b, d). High positive correlations between

the PNA index and cyclone frequency in the western subtropical Atlantic (up to 0.63) are observed during the last two decades only. Thus, variability in the cyclone frequency over the Gulf of Mexico and the east American coast was primarily associated with NAO during the period 1958–1978 and with PNA during the last two decades. Taking into account that the NAO shows a primarily negative correlation with PNA during the period 1979–1999, the PNA could be responsible for the maintenance in this region of the cyclone anomalies anticorrelated to the anomalies over the American continent and Arctic as demonstrated by the first Atlantic EOF (Fig. 8a).

There are several lines for the future development of this work. Our results provide a good opportunity for improving automated storm tracking algorithms that will be less biased in comparison to the semi-manual tracking. An important issue is the sensitivity of cyclone climatologies to the space-time resolution and the choice of different data sets. Blender and Schubert (2000) report considerable changes in the storm statistics derived from analyses with different space-time resolution. Quantification and possible parametrization of these effects may have profound implications for the further use of the SLP archives of centennial continuity (e.g., Trenberth and Paolino 1980), which have, however, coarse space-time resolution, at least for the earlier decades. In addition the comparative assessments, our results can provide links between variability in the cyclone frequency and results based on bandpass statistics of SLP and 500 hPa height, traditionally used to depict the storm tracks. Although bandpass statistics provide an effective measure of the intensity of synoptic scale processes, they account for both changing storms frequency and variations in the features of life cycle. Joint consideration of cyclone climatologies and bandpass statistics will help to quantify the contributions of these two effects. Cyclone statistics may be very effective for both analysis of atmospheric responses to ocean signals and for consideration of the changes at the sea-air interface forced by the atmosphere. For example, Gulev and Hasse (1999) showed that increasing significant wave heights in the North Atlantic (Bacon and Carter 1991) are associated with changing wind forcing frequency rather than with mean wind speed.

Acknowledgements We thank Glenn White of NCEP (Camp Spring) and Rolland Sweitzer of CDC (Boulder) who provided the NCEP/NCAR reanalysis data. Many thanks to Thomas Jung and Eberhard Ruprecht of IFM (Kiel), Evgenia Kalnay of the University of Maryland, Mark Serreze of the University of Colorado (Boulder), and Evgeniy Semenov of Moscow State University for helpful discussions. Technical help of Irina Rudeva, Julia Ziuliaeva, and Alexander Vakhrushin is greatly appreciated. We thank both anonymous reviewers for extremely helpful comments and Prof. Larry Gates for his editorial assistance. This work was supported by the Russian Foundation for Basic Research (grants 64-607, 64-656), the Volkswagen Stiftung (Project "North Atlantic Oscillation: Regional Impacts on European Climate"), and the EU INTAS Foundation, Brussels (grant 98-2089). This is a part of the PhD dissertation of OZ, who also had support from Moscow State University.

References

Agee EM (1991) Trends in cyclone and anticyclone frequency and comparison with periods of warming and cooling over the Northern Hemisphere. J Clim 4: 263–267

Alpert PB, Neeman U, Shau-El Y (1990a) Interannual variability of cyclone tracks in the Mediterranean. J Clim 3: 1474–1478

Alpert PB, Neeman U, Shau-El Y (1990b) Climatological analysis of Mediterranean cyclones using ECMWF data. Tellus 42A: 65–77

Ayrault F, Lalaurette F, Joly A, Loo C (1995) North Atlantic ultra high frequency variability. Tellus 47A: 671–696

Bacon S, Carter DJT (1991) Wave climate changes in the North Atlantic and North Sea. Int J Climatol 11: 545–588

Barnston AG, Livezey RE (1987) Classification, seasonality and persistence of low-frequency atmospheric circulation patterns. Mon Weather Rev 115: 1083–1126

Bell GD, Bosart LF (1989) A 15-year climatology of Northern Hemisphere 500 mb closed cyclone and anticyclone centers. Mon Weather Rev 117: 2142–2162

Blackmon ML, Lee YH, Wallace JM, Hsu HH (1984) Horizontal structure of 500 mb height fluctuations with long, intermediate and short time scales. J Atmos Sci 41: 961–979

Blender R, Schubert M (2000) Cyclone tracking in different spatial and temporal resolutions. Mon Weather Rev 128: 377–384

Blender R, Fraedrich K, Lunkeit F (1997) Identification of cyclone track regimes in the North Atlantic. Q J R Meteorol Soc 123: 727–741

Branstator G (1995) Organization of storm track anomalies by recurring low-frequency circulation anomalies. J Atmos Sci 52: 207–226

Carnell RE, Senior CA (1998) Changes in mid-latitude variability due to increasing greenhouse gases and sulphate aerosols. Clim Dyn 14: 369–383

Carnell RE, Senior CA, Mitchell JFB (1996) An assessment of measures of storminess: simulated changes in northern hemisphere winter due to increasing CO_2. Clim Dyn 12: 467–476

Chandler M, Jonas J (1999) Atlas of extratropical cyclones (1961–1998). NASA Goddard Institute for Space Studies and the Center for Climate System Research at Columbia University. New York, NY, USA

Christoph M, Ulbrich U (2000) Can NAO-PNA relationship be established via the North Atlantic storm track? Geophys Res Abstr 2: 215

Christoph M, Ulbrich U, Speth P (1997) Midwinter suppression of Northern Hemisphere storm track activity in the real atmosphere and in GCM experiments. J Atmos Sci 54: 1589–1599

Dickson RR, Namias J (1976) North American Influences on the circulation and climate of the North Atlantic sector. Mon Weather Rev 104: 1255–1265

Grigoriev S, Gulev SK, Zolina O (2000) Innovative software facilitates cyclone tracking and analysis. Eos Trans 81: 170

Gulev SK (1997) Climate variability of the intensity of synoptic processes in the North Atlantic midlatitudes. J Clim 10: 574–592

Gulev SK, Hasse L (1999) Changes of wind waves in the North Atlantic over the last 30 years. Int J Climatol 19: 720–744

Gulev SK, Zolina O, Reva Y (2000) Synoptic and sub-synoptic variability in the North Atlantic as revealed by the Ocean Weather Station data. Tellus 52A: 323–329

Harold JM, Bigg GR, Turner J (1999) Mesocyclone activity over the northeast Atlantic. Part 1: vortex distribution and variability. Int J Climatol 19: 1187–1204

Hayden BP (1981a) Secular variations in Atlantic coast extratropical cyclones. Mon Weather Rev 109: 159–167

Hayden BP (1981b) Cyclone occurrence mapping: equal area or raw frequencies. Mon Weather Rev 109: 168–172

Hilmer M, Jung T (2000) Evidence for a recent change in the link between the North Atlantic Oscillation and Arctic sea ice. Geophys Res Lett 27: 989–992

Hodges KI (1994) A general method for tracking analysis and its application to meteorological data. Mon Weather Rev 122: 2573–2586
Hurrell JW (1995) Decadal trends in the North Atlantic Oscillation: regional temperatures and precipitation. Science 269: 676–679
Hurrell JW, van Loon H (1997) Decadal variations in climate associated with the North Atlantic Oscillation. Clim Change 36: 301–326
Jones DA, Simmonds I (1993) A climatology of Southern Hemisphere extratropical cyclones. Clim Dym 9: 131–145
Kalnay E, et al (1996) The NCEP/NCAR 40-year reanalysis project. Bull Am Meteorol Soc 77: 437–471
Kodera K, Koide H, Yoshimura H (1999) Northern Hemisphere winter circulation associated with the North Atlantic Oscillation and stratospheric polar night jet. Geophys Res Lett 26: 443–446
Koenig WR, Sausen R, Sielmann F (1993) Objective identification of cyclones in GCM simulations. J Clim 6: 2217–2231
Kushnir Y (1994) Interdecadal variations in North Atlantic sea surface temperature and associated atmospheric conditions. J Clim 7: 142–157
Kushnir Y, Wallace JM (1989) Low-frequency variability in the Northern Hemisphere winter: geographical distribution, structure and time scale. J Atmos Sci 46: 3122–3142
Lambert S (1996) Intense extratropical Northern Hemisphere winter cyclone events: 1899–1991. J Geophys Res 101: 21319–21325
Le Treut H, Kalnay E (1990) Comparison of observed and simulated cyclone frequency distribution as determined by an objective method. Atmosfera 3: 57–71
Murray RJ, Simmonds I (1991) A numerical scheme for tracking cyclone centres from digital data. Part I: development and operation of the scheme. Aust Meteorol Mag 39: 155–166
NCEP (2000) Reanalysis PSFC problem 1948–1967. Internal note. Available at http://lnx21.wwb.noaa.gov/images/psfc/psfc.html
Osborn TJ, Briffa KR, Tett SFB, Jones PD, Trigo RM (1999) Evaluation of the North Atlantic Oscillation as simulated by a coupled climate model. Clim Dyn 15: 685–702
Reitan CH (1974) Frequency of cyclones and cyclogenesis for North America. 1951–1970. Mon Weather Rev 102: 861–868
Roebber PJ (1984) Statistical analysis an updated climatology of explosive cyclones. Mon Weather Rev 112: 1577–1589
Roebber PJ (1989) On the statistical analysis of cyclone deepening rates. Mon Weather Rev 117: 2293–2298
Rogers JC (1984) The association between the North Atlantic Oscillation and the Southern Oscillation in the Northern Hemisphere. Mon Weather Rev 112: 1999–2015
Rogers JC (1997) North Atlantic storm track variability and its association to the North Atlantic Oscillation and climate variability in the Northern Europe. J Clim 10: 1635–1647
Rogers E, Bosart LF (1986) An investigation of explosively deepening oceanic cyclones. Mon Weather Rev 114: 702–718
Sanders F (1986) Explosive cyclogenesis in the West–Central North Atlantic Ocean, 1981–1984. Part I. Composite structure and mean behaviour. Mon Weather Rev 114: 1781–1794
Sanders F, Gyakum JR (1980) Synoptic-dynamic climatology of the "bomb". Mon Weather Rev 108: 1589–1606
Schinke H (1993) On the occurrence of deep cyclones over Europe and the North Atlantic in the period 1930–1991. Beitr Phys Atmos 66: 223–237
Schubert M, Perlwitz J, Blender R, Fraedrich K, Lunkeit F (1998) North Atlantic cyclones in CO2-induced warm climate simulations: frequency, intensity and tracks. Clim Dyn 14: 827–837
Serreze MC (1995) Climatological aspects of cyclone development and decay in the Arctic. Atmosphere–Ocean 33(1): 1–23
Serreze MC, Barry RG (1989) Synoptic activity in the Arctic basin, 1979–85. J Clim 1: 1276–1295
Serreze MC, Box JE, Barry RG, Walsh JE (1993) Characteristics of Arctic synoptic activity, 1952–1989. Meteorol Atmos Phys 51: 147–164
Serreze MC, Carse F, Barry RG, Rogers JC (1997) Icelandic low cyclone activity: climatological features, linkages with the NAO, and relationships with the recent changes in the northern hemisphere circulation. J Clim 10: 453–464
Sickmoeller M, Blender R, Fraedrich K (2000) Observed winter cyclone tracks in the Northern hemisphere in re-analysed ECMWF data. Q J R Meteorol Soc 126: 591–620
Simmonds I, Keay K (2000) Variability of Southern Hemisphere extratropical cyclone behaviour, 1958–1997. J Clim 13: 550–561
Sinclair MR (1994) An objective cyclone climatology for the Southern Hemisphere. Mon Weather Rev 122: 2239–2256
Sinclair MR (1997) Objective identification of cyclones and their circulation, intensity and climatology. Weather Forecast 12: 591–608
Sinclair MR, Watterson IG (1999) Objective assessment of extratropical weather systems in simulated climates. J Clim 12: 3467–3485
Stein O, Hense A (1994) A reconstructed time series of the number of extreme low pressure events since 1880. Meteorol Z NF3: 43–46
Stewart RE, Donaldson NR (1989) On the nature of rapidly deepening Canadian east coast winter storms. Atmosphere–Ocean 27(1): 87–107
Taylor KE (1986) An analysis of the biases in traditional cyclone frequency maps. Mon Weather Rev 114: 1481–1490
Tibaldi S, Buzzi A, Speranza A (1990) Orographic cyclogenesis. In: Newton CW, Holopainen EO (eds) Extratropical cyclones. The Eric Palmen memorial volume. AMS, Boston, pp 107–128
Trenberth KE (1991) Storm tracks in the Southern Hemisphere. J Atmos Sci 48: 2159–2178
Trenberth KE, Paolino DA (1980) The Northern Hemisphere sea-level pressure data set: trends, errors and discontinuities. Mon Weather Rev 108: 855–872
Trigo IF, Davies TD, Bigg GR (1999) Objective climatology of cyclones in the Mediterranean region. J Clim 12: 1685–1696
Uccellini LW (1990) Processes contributing to the rapid development of extratropical cyclones. In: Newton CW, Holopainen EO (eds) Extratropical cyclones. The Eric Palmen memorial volume. AMS, Boston, pp 81–106
Ueno K (1993) Interannual variability of surface cyclone tracks, atmospheric circulation patterns, and precipitation patterns in winter. J Meteorol Soc Japan 71: 655–671
Ulbrich U, Christoph M (1999) A shift of the NAO and increasing storm track activity over Europe due to anthropogenic gas forcing. Clim Dyn 15: 551–559
von Storch H, Zwiers FW (1999) Statistical analysis in climate research. Cambridge University Press, Cambridge, UK, pp 503
von Storch H, Guddal J, Iden KA, Jonsson T, Perlwitz J, Reistad M, de Ronde J, Schmidt H, Zorita E (1993) Changing statistics of storms in the North Atlantic. Max-Planck Institut Meteorol Rep 116, Hamburg, Germany, pp 19
Wallace JM, Smith C, Jiang Q (1990) Spatial patterns of atmosphere–ocean interaction in the Northern winter. J Clim 3: 990–998
White G (2000) Long-term trends in the NCEP/NCAR Reanalysis. Proc 2nd Int Conf on Reanalyses, Reading, England. World Meteorological Organization, Geneva, Switzerland
Whittaker LM, Horn LH (1981) Geographical and seasonal distribution of North American cyclogenesis, 1958–1977. Mon Weather Rev 109: 2312–2322
Yau MK, Jean M (1989) Synoptic aspects and physical processes in the rapidly intensifying cyclone of 6–8 March 1986. Atmosphere–Ocean 27: 59–86
Zishka KM, Smith PJ (1980) The climatology of cyclones and anticyclones over North America and surrounding ocean environs for January and July 1950–1977. Mon Weather Rev 108: 387–401

Appendix: assessment of the accuracy of the cyclone tracking

The semi-automatic tracking procedure may be influenced by errors introduced by a particular operator which can be interpreted as random observational errors. Although the 42-year production

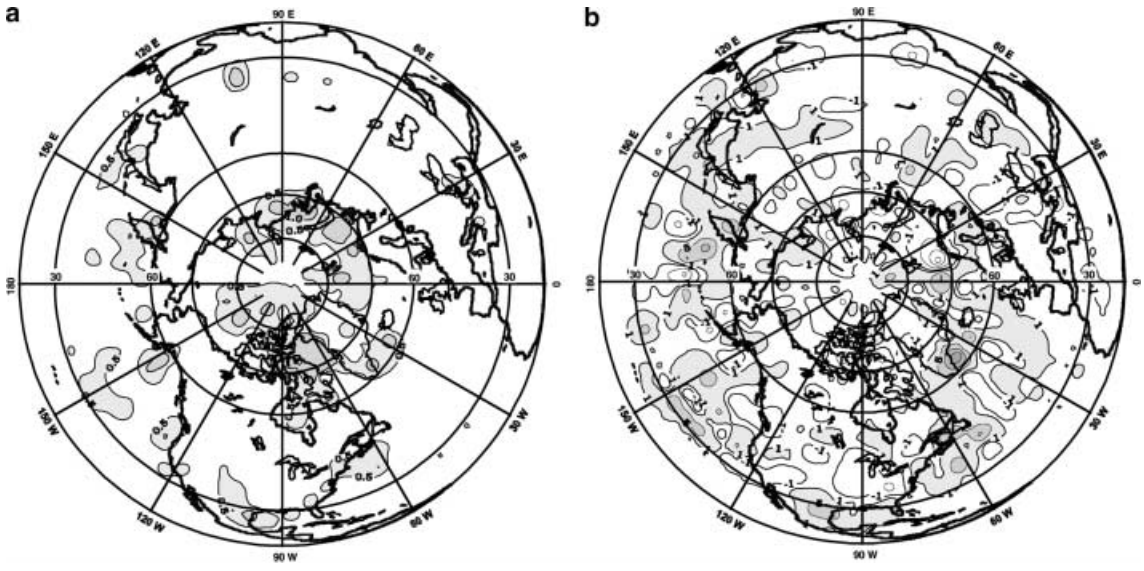

Fig. A1a, b Absolute variations (events per winter) of the cyclone frequency for 1993 computed from the storm tracking **a** performed by different operators, and **b** differences between the winter cyclone frequencies derived in this study and by the numerical tracking algorithm of Serreze (1995) for 1993

was performed by one operator (OZ), storm tracking for some winters was done independently by different operators. We can call $\boldsymbol{D}_{1,2} = |x_1 - x_2|$ the absolute variation between cyclone characteristics obtained by operators "1" and "2", and $\delta_{1,2} = \boldsymbol{D}_{1,2}/|x_2|$ the percentage of variation of results of operator "1" relative to the results of operator "2". For n operators $\langle \boldsymbol{D}_{i,j} \rangle = \sum_{i=1}^{n} \sum_{j=1}^{n} D_{i,j}/c_n^2$ and $\langle \delta_{i,j} \rangle = \sum_{i=1}^{n} \sum_{j=1}^{n} \delta_{i,j}/c_n^2$ exhibit mean absolute and relative operator-to-operator variations. Figure A1a shows estimates of the absolute variations in winter cyclone frequencies derived by four operators for 1993. In the storm formation and storm track regions errors range from 0 to 1 cyclone per winter, which corresponds to a relative error less than 5%. Accuracy in the Arctic is somewhat lower (largest relative error is about 10%). The local maximum in error in the Gulf of Alaska (5% relative variation) is connected with the difficulties in identification of the quasi-stationary systems. Errors over the Gulf coast result from uncertainty in identification of cyclogenesis in this region and may lead to the one cyclone per winter uncertainty. Thus, we can conclude that the average uncertainty of semi-manual tracking is about 2% and does not exceed 5% for most of regions.

Fully automated storm tracking algorithms usually underestimate *cyclone frequencies*, although they can overestimate *the number of cyclones*, identifying some centers of rapidly propagating or stationary lows as newly generated events. We employed the numerical scheme of Serreze (1995) which was used for the tracking of Arctic cyclones (e.g., Serreze et al. 1993, 1997). The FORTRAN code was supplied by Mark Serreze of the University of Colorado. We applied it to the tracking results derived using a numerical scheme with the same thresholds as for our data. Figure A1b shows winter differences in cyclone frequencies derived from a semi-automatic procedure (Grigoriev et al. 2000) and the Serreze (1995) scheme for 1993. Differences are nearly an order of magnitude higher than the operator-to-operator variation. Storm formation regions and storm track areas show 10 to 30% higher cyclone frequency in the semi-automatic procedure. However, open ocean regions may be characterized by higher frequencies derived from the numerical scheme, which inadequately interprets rapidly propagating and stationary lows. Remarkably, despite generally lower cyclone frequencies, the numerical procedure gives nearly 1.3 times more cyclones. Inspection of the statistics of cyclone lifetime indicates that this is due to the underestimation of lifetime. All numerical schemes give an artificial increase in cyclone frequency in mountain areas in southwest Asia. This results from the fact that numerical schemes identify here many short-lived orographic depressions, and form storm tracks linking newly generated local depressions. This region was excluded from our analysis. The same effect is observed over continental North America, where the numerical scheme gives higher cyclone frequency in comparison to semi-automatic tracking.

Numerical procedures tend to underestimate the frequency of intense cyclones and overestimate the frequency of shallow cyclones. Comparison of our results with the climatology of Chandler and Jonas (1999), who used 12-hourly NCEP/NCAR 1000 hPa height data and a simple numerical procedure than Serreze (1995), shows systematic underestimation of the frequency of deep cyclones by approximately 30 to 50%. Moreover, tracking schemes may underestimate cyclone lifetime and deepening rates, because the most intense deepening is often associated with rapid cyclone propagation, which may not be necessarily adequately interpreted. Thus, numerical schemes may introduce biases in both climatology and variability patterns. In this sense our results give the possibility to test and to improve the existing schemes and to develop new ones.